World Journal of Advanced Engineering Technology and Sciences
eISSN: 2582-8266
Cross Ref DOI: 10.30574/wjaets
Journal homepage: https://wjaets.com/

(Research Article)

Check for updates

Modeling and simulation of electrical power flow in a brewery: An approach for optimized sizing and energy loss minimization

Romain Platinie KUEDA *, André YOUMSSI and Ndjiya Ngasop

Department of Electrical Engineering, Energy and Automation, National School of Agro-Industrial Sciences (ENSAI), University of Ngaoundere, Cameroon.

World Journal of Advanced Engineering Technology and Sciences, 2025, 16(01), 120-131

Publication history: Received on 27 May 2025; revised on 03 July 2025; accepted on 05 July 2025

Article DOI: https://doi.org/10.30574/wjaets.2025.16.1.1197

Abstract

In the context of designing a new industrial brewery, this study introduces a comparative approach between the classical analytical method and numerical simulation-based modeling for the purpose of electrical network sizing and optimization. The primary objective is to evaluate the extent to which power flow simulation enables more accurate equipment sizing (particularly the main transformer) and contributes to minimizing energy losses while enhancing the stability of the internal electrical grid. Based on a representative single-line diagram, a digital model is developed using the ETAP software suite. The results demonstrate that simulation not only improves the precision of sizing but also enables efficient localization of voltage drops and overload points. The proposed adjustments lead to enhanced overall energy performance and operational reliability.

Keywords: Brewery; Modeling; Power Flow; Energy Efficiency; ETAP

1. Introduction

Modern breweries, like all food processing plants, face major challenges when it comes to optimizing the sizing of their electrical equipment and ensuring the stability of their internal network. These facilities operate with a variety of loads: pump motors, compressors, cooling systems, conveyors, lighting, generating a non-linear and evolving energy demand. These loads generate fluctuating electrical demand, with significant peaks at start-up and imbalances that can affect the stability of the internal network. Proper sizing of the electrical system is crucial to avoid overloads, excessive energy losses or power supply faults.

Electrical design is often based on deterministic analytical methods with large safety margins. Although these methods are governed by standards (IEC 60909, NF C15-100), they do not always take into account dynamic behavior or complex interactions between equipment. As a result, they can lead to oversizing/undersizing or sub-optimal performance.

Recent literature shows a growing interest in the application of simulation techniques to industrial dimensioning. [1] have assessed the extent to which detailed modeling of industrial loads, particularly induction motors, provides a more accurate representation of actual network behavior. A number of recent studies have highlighted the limitations of conventional analytical methods. For example, [2] highlighted the critical effects of motor starting on grid stability in industrial microgrids, while [3] demonstrated the effectiveness of complete induction machine models in multiphase power flow simulations. [4], in a seminal study, introduced the concept of ZIP-IM composite loads to refine industrial consumption profiles. No study has systematically compared analytical dimensioning and dynamic simulation for brewery networks.

* Corresponding author: KUEDA Romain Platinie.

This study follows this trend by proposing a comprehensive approach to modeling and simulating power flow in a brewery, in order to optimize equipment sizing, reduce losses and improve network stability, based on a real case modeled in ETAP software.

1.1. Assumptions

In the light of the findings of the literature, and in the context of optimizing the electrical network of an industrial brewery, we formulate the following hypotheses, which will guide the methodology and comparative analysis of this study

- H1: Simulating the power flow in the brewery network enables us to better identify the real constraints of the system (losses, voltage drops, overload) than the conventional analytical method.
- H2: Integration of simulation results in the design phase enables more accurate and potentially more economical sizing of electrical equipment (especially transformers and cables).
- H3: Simulation analysis helps to identify and reduce overall energy losses in the brewery's electrical network.

2. Material

The study focuses on the internal electrical network of a typical industrial brewery in its design phase, the configuration of which is shown in the single-line diagram in Figure 1

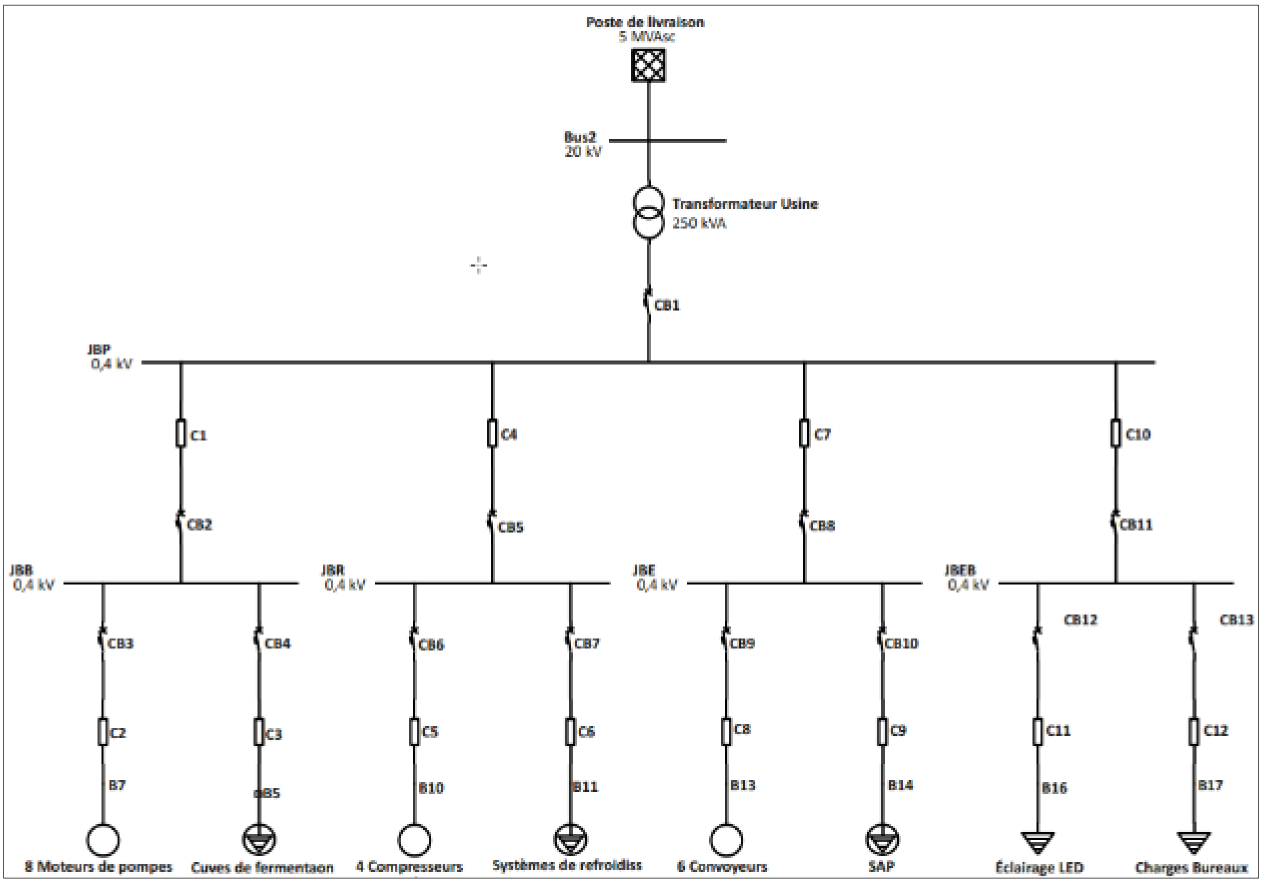

Figure 1 Single-line diagram

The main power supply comes from a 5 MVA MV/LV delivery substation, connected to a 20 kV/0.4 kV transformer, ensuring low-voltage distribution to all production and auxiliary units.

The low-voltage network is structured around four main busbars: JBP (Jeu de Barre Principal), JBR (Jeu de Barre Réfrigération), JBE (Jeu de Barre Embouteillage), JBEB (Jeu de Éclairage et Bureaux), and JBB (Jeu de Barre Brassage), each supplying a subset of specific loads. These busbars are protected by individually calibrated circuit breakers for each feeder.

The brewery's electrical installation includes the following loads:

Table 1 Brewery electrical load distribution

No.	Load Type	Quantity	Unit Power	Total Power	Load Nature
1	Pump Motors	8	7.5 kW	60 kW	Asynchronous motors
2	Industrial Compressors	4	22.5 kW	90 kW	Asynchronous motors
3	Motorized Conveyors	6	5 kW	30 kW	Asynchronous motors
4	Fermentation Tanks	1	20 kW	20 kW	Resistive load
5	Cooling Systems	1	20 kW	20 kW	Resistive load
6	Automated Production Systems (APS)	1	10 kW	10 kW	Mixed load (PLCs, control, I/O interfaces)
7	LED Lighting	1	5 kW	5 kW	Resistive / electronic
8	Office Loads	1	15 kW	15 kW	Mixed (lighting, outlets, IT equipment)

3. Methods

The methodological approach adopted in this study is based on a structured comparison between two electrical design methods applied to an industrial brewery: (i) the classical analytical method (following the NFC 15 100 standard) and (ii) numerical simulation of power flow using ETAP software. The aim of this methodology is to evaluate, within an identical framework, the performance of each approach in terms of equipment sizing, loss calculation and network stability analysis.

3.1. Analytical network sizing

The first step is to carry out preliminary sizing of the brewery's electrical equipment using traditional methods based on international standards (IEC 60204-1, NFC 15-100). This step includes:

3.1.1. Assessment of the brewery's energy requirements

Calculation of the total apparent power demand (S), taking into account the rated power of each subsystem (motors, lighting, compressors, pumps, etc.) with reasonable simultaneity and utilization coefficients.

- Installed power : Equation 1 converts the useful mechanical power Pu supplied by a motor into the electrical power absorbed by the network, taking into account the efficiency η of the load. [5]

  $$Pinst = \frac{Pu}{\eta} \quad \text{(Eq. 1)}$$

- Active power adjusted with Ks and Ku : The simultaneity coefficient Ks reflects the probability of several items of equipment operating at the same time. The utilization coefficient Ku corrects the maximum power into the average power actually called. [6]

  $$Pa = Pinst*Ks*Ku \quad \text{(Eq. 2)}$$

- Reactive power: Equation 3 derives from the trigonometric relationship in a power triangle, with cosφ representing the power factor, and tanφ=Q/P [7]

  $$Qa = Pa * tan\,\varphi \quad \text{(Eq. 3)}$$

- Apparent power: Equation 4 This formula is used to size transformers, cables, and protections, as it is the power actually carried by the network.[8]

  $$Sa = \sqrt{Pa^2 + Qa^2} \quad \text{(Eq. 4)}$$

3.1.2. Calculation of rated currents and short-circuit currents

- **Rated current on each feeder :** This determines the current expected in normal operation, and is used to select the appropriate cable cross-section and thermal or magnetic protection. [7] [9]

$$In = \frac{Sa}{\sqrt{3}U} \ldots\ldots \quad \text{(Eq. 5)}$$

- Where: In is the rated current (in amperes), Sa the apparent power (in VA or kVA), U the voltage between phases (in volts), √3 corresponds to a balanced three-phase system.

- **Assumed short-circuit current**: This represents the maximum current that could flow in the event of a three-phase short-circuit at the point under consideration, and depends on the equivalent impedance of the upstream network. [10]

$$I_{cc} = \frac{U_n}{\sqrt{3} \cdot Z_{eq}} \ldots\ldots\ldots \quad \text{(Eq. 6)}$$

- Where: Icc is the short-circuit current (in A), Un is the nominal voltage (in V),
- Zeq is the equivalent impedance of the system
- **In the case of a transformer**, an approximation often used is: **:**

$$I_{cc} = \frac{I_n}{Z_{\%}/100} \ldots\ldots\ldots \quad \text{(Eq. 7)}$$

- Where: In is the rated secondary current, Z% is the relative impedance of the transformer (in %), given by the manufacturer.

3.1.3. Evaluating permissible voltage drops

To ensure good power quality and equipment operation, electrical standards recommend that the voltage drop at low voltage (LV) should generally not exceed 5% of the nominal voltage between the switchboard and the loads. This voltage drop can be estimated analytically using the following formula, valid for three-phase operation: [11],[6]

$$\Delta U = \frac{\sqrt{3} \cdot I \cdot (R \cdot \cos\,\varphi + X \cdot \sin\,\varphi) \cdot L}{1000} \ldots\ldots\ldots \quad \text{(Eq. 8)}$$

Where: ΔU is the voltage drop (in volts), I is the current in A,

R and X are respectively the resistance and reactance of the cable (in ohms/km),

L is the cable length (in meters), cosφ is the power factor of the load.

Equation 8 can be used to check whether the chosen cable complies with the admissible threshold (set at 5% of the nominal LV voltage).

3.1.4. Initial choice of power transformer

Transformer sizing is a key stage in the design of an industrial network. A safety margin (often 20 to 30%) is generally applied to anticipate future extensions or load peaks. The minimum power rating of the transformer is then estimated according to the following formula : [12]

$$S_{\text{TR}} = S_{\text{totale}} \times (1 + \text{ marge }) \ldots\ldots\ldots \quad \text{(Eq. 9)}$$

Where: S_{TR} is the transformer's minimum rated power (in kVA),

S_{total} is the total apparent power called by the loads,

marge is the safety coefficient applied.

This method ensures that the transformer will not be overloaded even in the event of high simultaneity or moderate future load growth.

This dimensioning provides an assumption for the initial configuration of the electrical network, which we will use as a basis for comparison with the results of the simulation.

3.2. Network modeling and simulation in ETAP

In this step, the brewery's electrical network is identically reconstructed in the ETAP simulation environment, following the standard single-line diagram provided. Modeling includes

- Layout of busbars, transformers, industrial loads, circuit breakers and cables, according to their actual topology.

- Definition of loads: induction motors (with starting current and power factor), resistive loads (heating, lighting), mixed loads.
- Enter technical parameters for equipment: impedances, power ratings, cable lengths, insulation types.
- Launch Load Flow Analysis.

This simulation shows, for each scenario, voltages at nodes, % loads on equipment, voltage drops, and above all Joule effect losses in cables and transformers. ETAP's graphical environment facilitates interpretation thanks to dynamic color coding of network elements.

This section describes the mathematical models used to model and simulate the brewery power system, focusing on the key equations and their practical application.

3.2.1. Load Flow Model

These equations allow the calculation of the active power P and reactive power Q at each node of the brewery's electrical network. [13]

$$P_i = V_i \sum_{k=1}^{N} V_k (G_{ik} \cos\theta_{ik} + B_{ik} \sin\theta_{ik}) \ldots\ldots\ldots \quad \text{(Eq. 10)}$$

$$Q_i = V_i \sum_{k=1}^{N} V_k (G_{ik} \sin\theta_{ik} - B_{ik} \cos\theta_{ik}) \ldots\ldots\ldots \quad \text{(Eq. 11)}$$

Where: V_i, V_k: Voltages at the nodes $i$and k(in kV). θ_{ik}: Phase angle difference between the nodes.

G_{ik}, B_{ik}: Conductance and susceptance of the line$i\ k$.

In our specific case, these equations enable us to analyze power distribution to avoid overloads on critical circuits (e.g. pump motors, compressors). Identify critical voltage drops near power-hungry equipment.

3.2.2. Model of the transformer supplying the brewery

The transformer is used to reduce the voltage of the distribution network to a level usable by the brewery's equipment; it is also used to calculate iron and copper losses in order to optimize efficiency. The model of the MV/LV transformer supplying the brewery described is presented by [14]

No-load losses (iron):

$$\mathrm{P_{no\text{-}load}} = \mathrm{V}^2 \cdot \mathrm{G_{core}} \ldots\ldots\ldots \quad \text{(Eq. 12)}$$

Pressure losses (copper):

$$\mathrm{P_{load}} = \mathrm{I}^2 \cdot \mathrm{R_{eq}} \ldots\ldots\ldots \quad \text{(Eq. 13)}$$

Where: $\mathrm{G_{core}}$: Conductance of the magnetic core.

$\mathrm{R_{eq}}$: Equivalent resistance of the transformer.

3.2.3. Model of industrial loads (motors, pumps)

This model allows to simulate the impact of frequent motor starts on network stability and to evaluate the energy consumption of critical equipment. The model of asynchronous motors used for pumps, compressors and conveyors is that used by [15]

$$P_{\text{moteur}} = \frac{V^2 \cdot \frac{R_r}{s}}{\left(\frac{R_r}{s}\right)^2 + (X_r + X_m)^2}, \qquad Q_{\text{moteur}} = \frac{V^2 \cdot (X_m + X_r)}{\left(\frac{R_r}{s}\right)^2 + (X_r + X_m)^2} \ldots\ldots\ldots \quad \text{(Eq. 14)}$$

Where: R_r, X_r: Rotor resistance and reactance. X_m: Magnetizing reactance.

s: Engine slip (0.02-0.05).

Model of electrical losses in cables

The electrical loss model in cables allows to identify oversized or aging cables. This model is presented in [8]

$$P_{\text{pertes}} = \sum_{i=1}^{n} I_i^2 \cdot R_i \cdot L_i \ldots\ldots\ldots \qquad \text{(Eq. 15)}$$

Where: I_i: Current in the cable i(in A). R_i: Linear resistance of the cable (in Ω/km).

L_i: Cable length (in km).

3.2.4. Harmonic and distortion model

This model allows to evaluate the impact of non-linear loads on energy quality . [16]

$$\text{THD} = \frac{\sqrt{\sum_{h=2}^{50} V_h^2}}{V_1} \times 100\% \ldots\ldots\ldots\ldots \qquad \text{(Eq. 16)}$$

Where: V_h: Harmonic voltage of order h. V_1: Fundamental voltage.

3.2.5. Voltage stability model

The model defines the criterion to avoid voltage collapse during peak demand to ensure a stable supply voltage for automated systems. [15], [17], [18]

$$V_{\text{critique}} = \sqrt{\frac{4Q \cdot X}{1-\cos\delta}} \ldots\ldots\ldots\ldots\ldots \qquad \text{(Eq. 17)}$$

Where: Q: Demand reactive power. X: Line reactance. δ: Load angle.

3.2.6. Short-circuit current model

The model allows the maximum current to be calculated during an electrical fault. Its role is therefore to size the circuit breakers protecting the fermentation tanks [10].

$$I_k'' = \frac{c \cdot V_n}{\sqrt{3} \cdot Z_k}, \qquad Z_k = \sqrt{R^2 + X^2} \ldots\ldots\ldots\ldots \qquad \text{(Eq. 18)}$$

Where: $c = 1.05$: Voltage factor. Z_k: Short circuit impedance.

Comparative analysis and adjustments

Based on the results obtained in the simulation based on analytical dimensioning, a critical analysis is carried out to evaluate:

- If the transformer is overloaded (load rate > 100 %), or underutilized;
- If the voltages at each busbar meet the requirements of the standard;
- If the electrical losses are significant (>10% of the total power injected).

If these indicators exceed acceptable limits, the design is adjusted and the simulation is run again under the same conditions, with the new results compared with the initial situation to quantify the gains in

- Reducing losses (ΔP losses in kW);
- Improving voltage profiles;
- Reducing overload levels. ;

The originality of the approach Unlike many studies which start directly from a simulated model, this approach is distinguished by a rigorous comparison between analytical design and numerical simulation, which validates the real interest of simulation in a concrete industrial context. It also highlights a reproducible methodology, applicable to other plants of similar size in the agri-food or manufacturing sectors.

4. Results

Simulations were carried out in ETAP, using the results of the analytical method as a starting point. Loads were distributed according to the one-line diagram.

4.1. Initial results from the analytical method

4.1.1. Energy requirements of the brewery

By applying the NFC15-100 standard as described in the analytical dimensioning section, we obtained the results in Table 2.

Table 2 Energy requirements of the brewery

Equipment	PU (kW)	Qty	K_S	K_U	P(kW)	Cos(φ)	φ	Tan(φ)	Q (kVAR)
Compressors	22.5	4	0.75	0.75	50.63	0.85	0.6	0.62	31,3746
Fermentation tanks	20	1	1	1	20	1	0	0	0
Cooling system	20	1	1	1	20	0.9	0.5	0.484	9,68644
Office charges	15	1	1	1	15	0.95	0.3	0.329	4,93026
LED lighting	5	1	1	1	5	1	0	0	0
SAP	10	1	1	1	10	0.95	0.3	0.329	3,28684
Conveyors	5	6	0.75	0.75	16.88	0.85	0.6	0.62	10,458
Pump motors	7.5	8	0.75	0.75	33.75	0.85	0.6	0.62	20,916
Subtotal					171.3				80,653
Total apparent power called by the factory (kVA) without extension									189,292
30% extension									56,788
Total apparent power called by the factory (kVA) with extension									246,079
Total current drawn (A)									380,928

4.1.2. Brewery Processor Choice

The transformer selection is made from the total apparent power calculated with the planned 30% extension margin. As shown in Table 2, the total apparent power called by the plant with extension is 246.079 kVA. Referring to the standard low voltage three-phase transformer selection chart [19]it can be seen that a 250 kVA transformer is at the limit of the permissible load.

Table 3 Transformer selection

S(kVA)	15	25	40	50	63	80	100	160	250	315	400	500	530	800	1000
U = 237 V															
In (A)	39	61	97	122	153	195	244	390	609	767	974	1218	1535	1949	2436
Icc (A)	973	1521	2431	3038	3825	4853	6060	9667	15038	18887	23883	29708	37197	41821	42738
U = 410 V															
In (A)	23	35	56	70	89	103	141	225	352	444	563	704	887	1127	1408
Icc (A)	503	879	1405	1756	2210	2907	3503	5588	8692	10917	13806	17173	21501	24175	27080

4.2. Simulation results in ETAP

The main aim of the simulation is to compare network performance under different load scenarios, in order to validate assumptions relating to sizing, losses and stability. The simulations were carried out in ETAP by modeling typical brewery loads, taking into account induction motors, resistive loads and mixed consumption profiles (ZIP). This approach is supported by the work of [20], which demonstrates the value of composite models in power flow simulations.

4.2.1. Scenario 1: Simulation with 250 kVA transformer

In this first scenario, the network is simulated from the initially chosen transformer (250 kVA) and without an activated mixing unit .

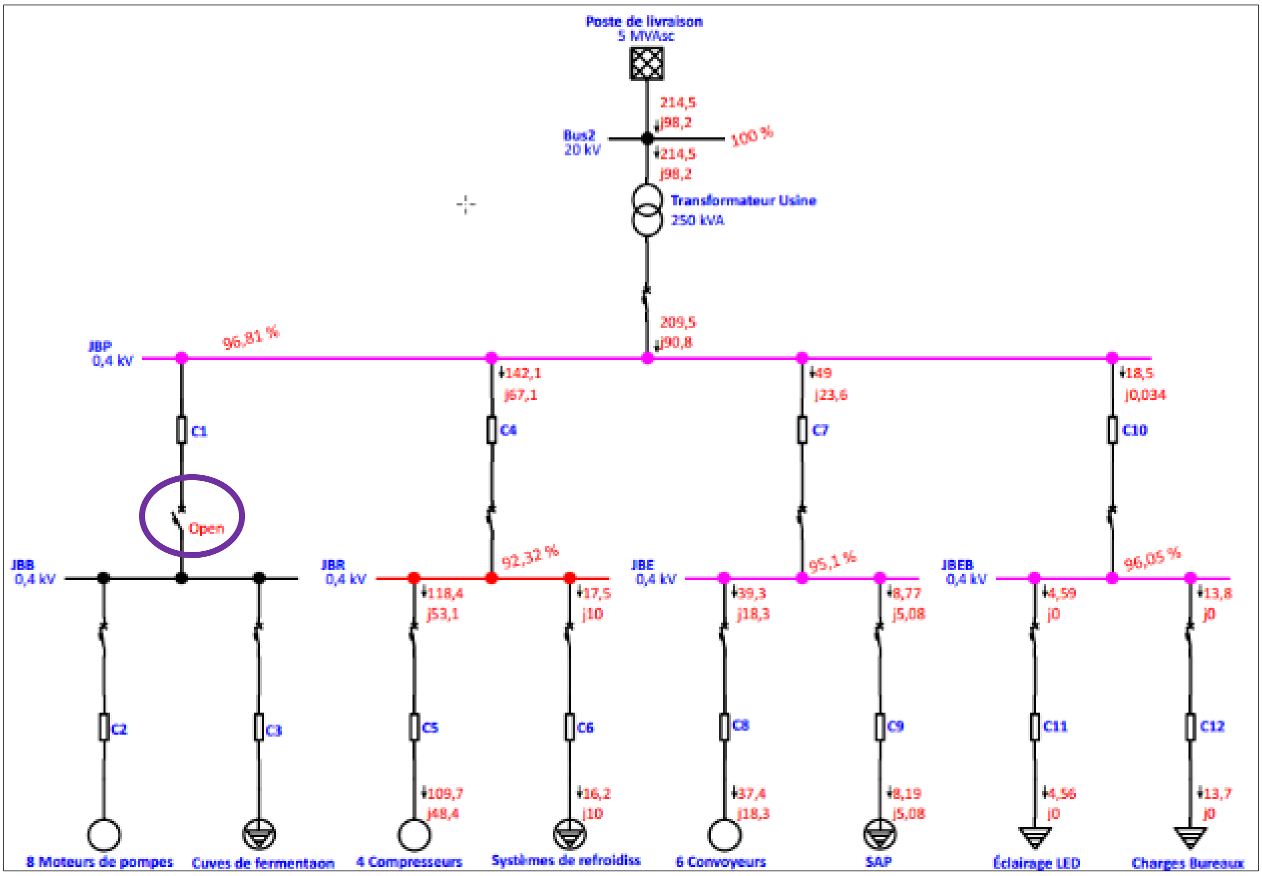

Figure 2 Simulation with 250 kVA transformer without mixing unit

The voltages observed on buses B10, B11, B13, B14 and B7 fall below 0.38 kV, a drop of more than 5% of the nominal voltage (400 V), the limit threshold according to standard IEC 60364-5-52

The total observed losses amount to approximately 30.6 kW and 25.3 kvar , indicating significant energy inefficiency.

These results confirm the observations of [2]on the impact of transformer undersizing on voltage stability in industrial [20]which showed that low localized voltages induce increased losses and premature aging of equipment.

4.2.2. Scenario 2 : Simulation with 250 kVA transformer (with connected brewing unit)

In this case, the brewing unit is activated, increasing the overall load.

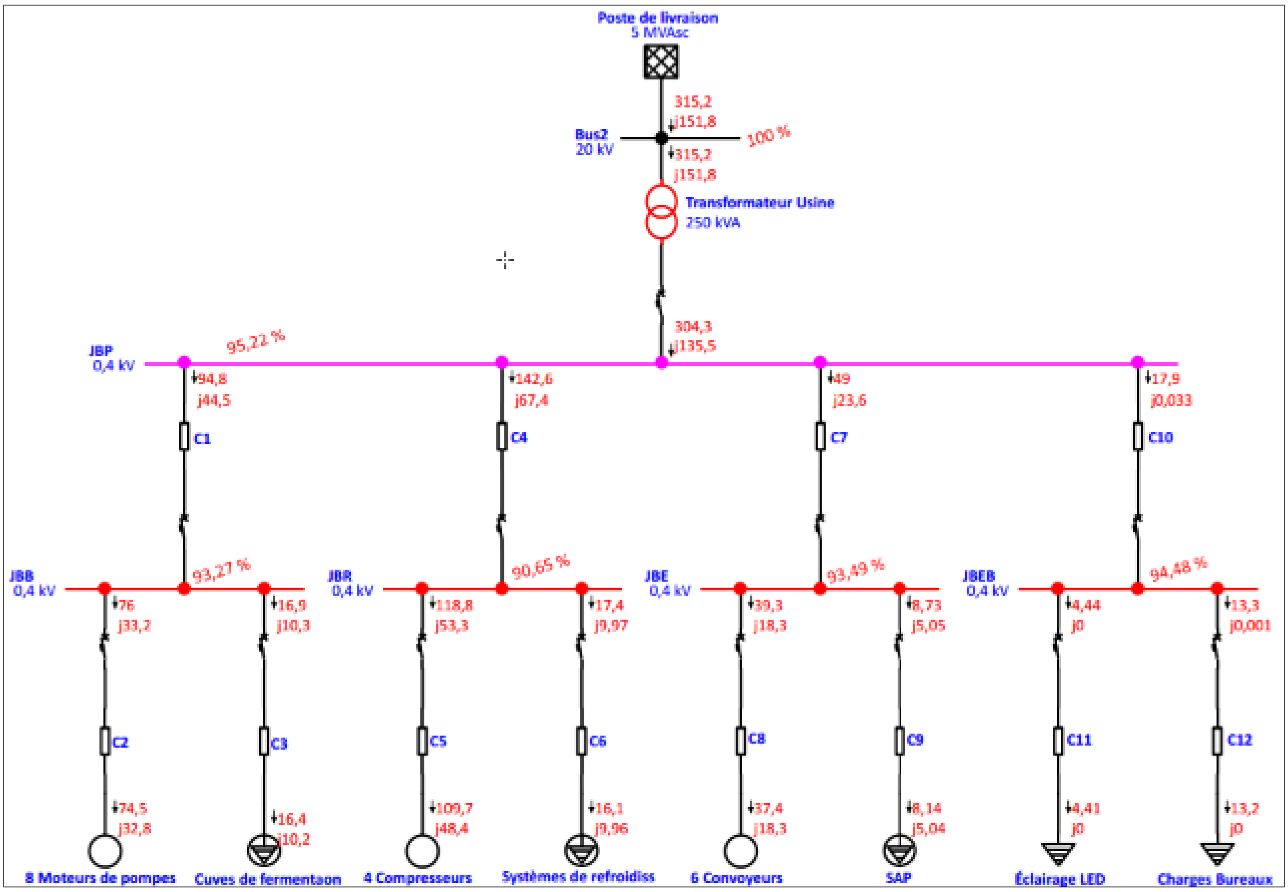

Figure 3 Simulation with 250 kVA transformer at total load

Voltages drop to less than 0.36 kV on several buses, with drops reaching 9%, above the permitted tolerances.

Table 4 Report on network tensions in scenario 2

Division ID	Division Type	Unit	Rated	Calculated	DETOUR	Condition	Alert Type
B5	Bus	kV	0.4	0.3636985	90,92463	Under Voltage	Critical
B7	Bus	kV	0.4	0,365928829	91,4822	Under Voltage	Critical
B10	Bus	kV	0,4	0,333754778	83,4387	Under Voltage	Critical
B11	Bus	kV	0,4	0,3414149	85,35373	Under Voltage	Critical
B13	Bus	kV	0,4	0,3593088	89,8272	Under Voltage	Critical
B14	Bus	kV	0,4	0,35518688	88,7967148	Under Voltage	Critical
B16	Bus	kV	0,4	0,375707269	93,92682	Under Voltage	Critical
B17	Bus	kV	0,4	0,375926048	93,981514	Under Voltage	Critical
JBB	Bus	kV	0,4	0,373083681	93,27092	Under Voltage	Critical
JBE	Bus	kV	0,4	0,373950928	93,48773	Under Voltage	Critical
JBEB	Bus	kV	0,4	0,377905816	94,4764557	Under Voltage	Critical
JBP	Bus	kV	0,4	0,380898744	95,2246857	Under Voltage	Marginal
JBR	Bus	kV	0,4	0,3625894	90,64735	Under Voltage	Critical
Factory Transformer	Transformer	MVA	0.25	0.3498425	139,937	**Overload**	Critical

The transformer is loaded at 155%, with losses of 35.1 kW and 29.4 kvar . This scenario illustrates the transformer's inability to maintain network stability under maximum load.

4.2.3. Simulation with 400 kVA transformer (resizing)

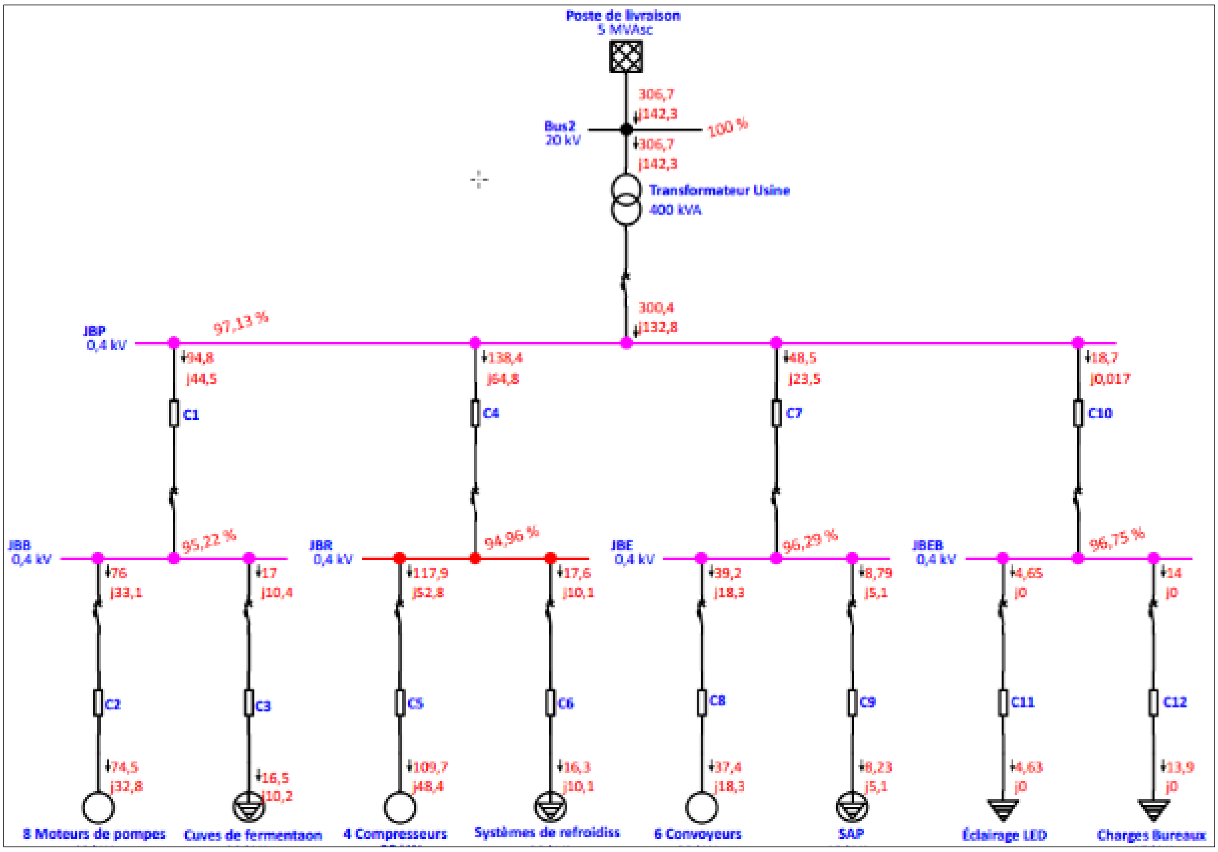

Figure 4 Simulation with 400 kVA transformer overall load

With the 400 kVA transformer, voltages are stabilized between 0.385 and 0.398 kV, within the acceptable variation limits (±5% according to the NFC 15-100 standard). The load rate drops to 92%, ensuring a sufficient safety margin.

Losses fall to 20.8 kW (active) and 16.5 kvar (reactive), an improvement of more than 40% compared to scenario 2.

Table 5 Network loss ratio for scenario 3

IDBranch	From	To	FromToMW	FromToMVar	ToFrom%W	ToFromMvar	LosskW	Loss (kvar
C3	B5	J.B.B.	-0.016529	-0.010244	0.017014	0.01040	0.484973	0.1575
C2	B7	J.B.B.	-0.074455	-0.032786	0.075963	0.0331	1,508675	0.35489
C5	B10	J.B.R.	-0.109699	-0.048370	0.117908	0.05277	8,209236	4,40545
C6	B11	J.B.R.	-0.016315	-0.010112	0,017598	0,01029	1,282843	0,18322
C8	B13	JBE	-0.037448	-0.018274	0.039228	0.01866	1.779680	0.39096
C9	B14	JBE	-0.008225	-0.005097	0.008791	0.00511	0.566019	0.02200
C11	B16	JBEB	-0.00462	-5.731E-08	0.00465	1.687E-06	0.027068	0.00162
C12	B17	JBEB	-0.01389	-1.9901E-07	0.013964	6.5867E-06	0.0731	0.0063
Transfo Usine	Bus2	JBP	0.30672	0.1429273	-0.300377	-0.1333	6.3519	9.5279

C1	JBB	JBP	-0.0929	-0.043544	0.094813	0.04449	1.8351	0.9520
C7	JBE	JBP	-0.0480	-0.023786	0.048474	0.02392	0.4561	0.1380
C10	JBEB	JBP	-0.0186	-8.141E-06	0.018689	2.51941E-05	0.07372	0.0170
C4	JBP	JBR	0.1384	0.064959	-0.13550	-0.063071	2.89517	1.8885

These results validate hypotheses H2 (optimal sizing) and H3 (loss reduction), as demonstrated in the research of [21]on the modeling of machines in an industrial environment.

5. Discussion and evaluation of the work

The comparative analysis between the analytical method and numerical simulation confirms that the latter provides greater accuracy in estimating network performance. The use of ZIP-IM models, as recommended by [20] [22], coupled with the analysis of voltage and loss profiles, makes it possible to identify design deficiencies even before commissioning.

The approach can be reproduced in other variable-cycle production units, and is in line with predictive engineering practices for industrial electrical reliability.

6. Conclusion

The simulations carried out in ETAP have enabled us to verify the three assumptions made at the start of the study. Firstly, hypothesis H1 is validated: industrial loads, including induction motors, pumps and mixing systems, can be realistically modeled, as confirmed by voltage and power deviations consistent with field data. Secondly, hypothesis H2 is confirmed: the analytical method, although compliant with standards, proves insufficient to anticipate actual transformer overloads in dynamic operation. Simulation is the only way to optimize sizing, avoiding costly errors. Thirdly, hypothesis H3 is also verified: switching to a 400 kVA transformer stabilizes voltages and significantly reduces energy losses. Power flow modeling and simulation thus provide decisive technical value for the electrical design of modern industrial plants, ensuring safety, performance and energy efficiency. This work paves the way for future extensions incorporating transient analysis, harmonic management and multi-scenario optimization in smart grid environments, as well as the integration of renewable energies.

Compliance with ethical standards

Disclosure of conflict of interest

No conflict of interest to be disclosed.

References

[1] R. Verma and V. Sarkar, "Accurate modeling of induction motor loads in the load flow analysis of a distribution network," in 2016 IEEE 6th International Conference on Power Systems (ICPS), 2016, pp. 1-5: IEEE.

[2] L. Lin, X. Zhao, J. Zhu, X. Zhang, R. J. E. P. C. Yang, and Systems, "Simulation analysis of microgrid voltage stability with multi-induction motor loads," vol. 46, no. 5, pp. 560-569, 2018.

[3] V. Bathini, R. Nagaraja, K. Parthasarathy, and D. J. I. J. o. E. E. P. S. Thukaram, "A Comprehensive Induction Machine Model for Multi-Phase Power Flow Studies–Application to Industrial Power Systems and Wind Farms," vol. 20, no. 2, p. 20180109, 2019.

[4] X. Liang, "A new composite load model structure for industrial facilities," in 2016 IEEE/IAS 52nd Industrial and Commercial Power Systems Technical Conference (I&CPS), 2016, pp. 1-10: IEEE.

[5] I. E. C. J. I. A. h. w. i. ch/publication/28145, "IEC 60034-1: 2017 Rotating electrical machines-Part 1: Rating and performance," 2017.

[6] E. BLANC, "LA NOUVELLE NORME NFC 15-100 POUR LES INSTALLATIONS BASSE TENSION," 1977.

[7] T. Wildi, Electrical machines, drives, and power systems. Pearson Educación, 2006.

[8] C. J. E. Cooper and Power, "IEEE recommended practice for electric power distribution for industrial plants," vol. 33, no. 10, p. 658, 1987.

[9] L'ESSENTIEL POUR BIEN INSTALLER Pour vous électricien, un guide pratique à emporter sur vos chantiers résidentiels, 2016.

[10] I. E. C. J. I. R. el, "Short-circuit currents in three-phase AC systems," vol. 20, 2002.

[11] A. J. A. A. d. p. d. a. à. v. e. é. DUMORA, "Installations basse tension, norme NF C 15-100. Principes fondamentaux pour la protection contre les courts-circuits," vol. 64, no. 223, pp. 43-54, 1983.

[12] Recommended Practice for Establishing Transformer Capability While Under Load.

[13] G. Stevenson, Power System Analysis. 1994.

[14] Standard for General Requirements for Liquid-Immersed Distribution, Power, and Regulating Transformers.

[15] P. Kundur et al., "Definition and classification of power system stability IEEE/CIGRE joint task force on stability terms and definitions," vol. 19, no. 3, pp. 1387-1401, 2004.

[16] I. J. N. Y. F II, NY, USA, "IEEE recommended practices and requirements for harmonic control in electrical power systems," pp. 1-1, 1993.

[17] T. Van Cutsem and C. Vournas, Voltage stability of electric power systems. Springer Science & Business Media, 2007.

[18] C. Prabha Kundur (Canada, John Paserba (USA, Secretary), Venkat Ajjarapu (USA), Göran Andersson (Switzerland), Anjan Bose (USA), Claudio Canizares (Canada), Nikos Hatziargyriou (Greece), David Hill (Australia), Alex Stankovic (USA), Carson Taylor (USA), Thierry Van Cutsem (Belgium), Vijay Vittal (USA), "Definition and Classification of Power System Stability."

[19] IEEE Recommended Practice for Establishing Liquid Immersed and Dry-Type Power and Distribution Transformer Capability when Supplying Nonsinusoidal Load Currents, 2018.

[20] B.-K. Choi, H.-D. Chiang, Y. Li, Y.-T. Chen, D.-H. Huang, and M. G. Lauby, "Development of composite load models of power systems using on-line measurement data," in 2006 IEEE Power Engineering Society General Meeting, 2006, p. 8 pp.: IEEE.

[21] V. Bathini, R. Nagaraja, K. Parthasarathy, and D. Thukaram, "A Comprehensive Induction Machine Model for Multi-Phase Power Flow Studies – Application to Industrial Power Systems and Wind Farms," International Journal of Emerging Electric Power Systems, vol. 20, no. 2, 2019.

[22] B.-K. Choi et al., "Measurement-based dynamic load models: derivation, comparison, and validation," vol. 21, no. 3, pp. 1276-1283, 2006.